Supplemental Information to: Thermoresponsive oil-continuous gels based on double-interpenetrating colloidal-particle networks

Braulio A. Macias-Rodriguez[a,b]*, Roland Gouzy[a], Corentin Coulais[a], Krassimir P. Velikov[a, b, c]*

[a]Institute of Physics, University of Amsterdam, Science Park 904, 1098 XH Amsterdam, The Netherlands

[b]Unilever Innovation Center, Bronland 14, 6708 WH Wageningen, The Netherlands

Dr. Braulio A. Macias-Rodriguez, Prof. Krassimir P. Velikov

[c]Soft Condensed Matter, Debye Institute for Nanomaterials Science, Utrecht University, Princetonplein 5, 3584 CC Utrecht, The Netherlands

*E-mail: bmacias1710@gmail.com, krassimir.velikov@unilever.com

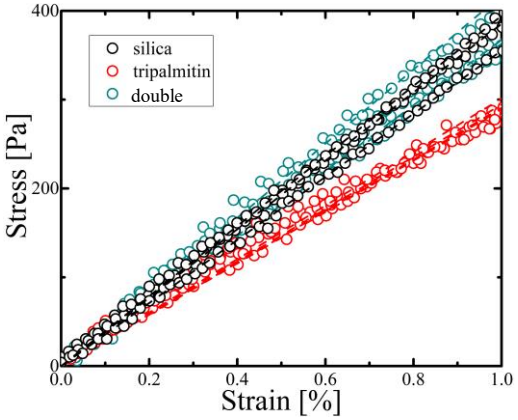

Figure S1. Trimmed curves showing the beginning of the second reloading cycle from which we derived the elastic moduli $S = \frac{d\sigma}{d\gamma}$ (dotted lines).

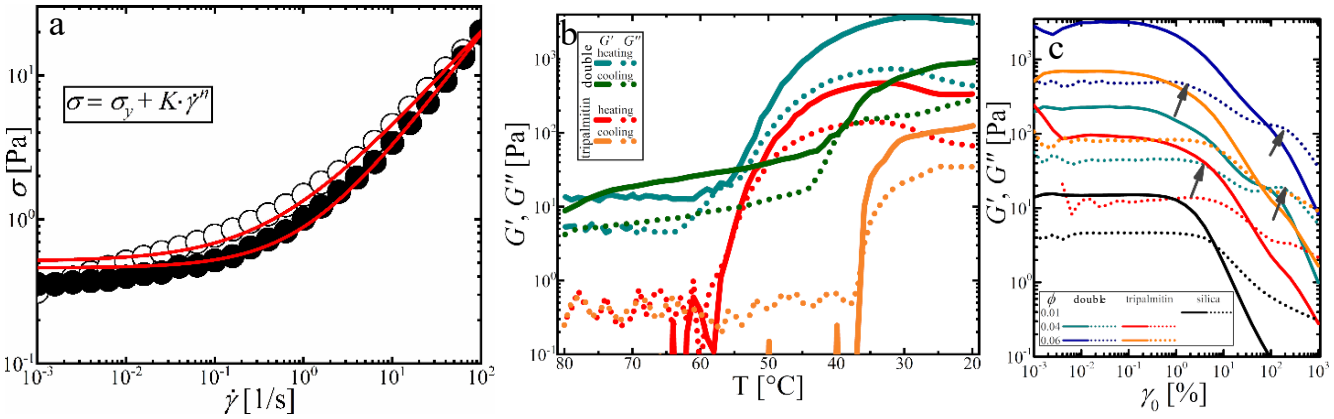

Figure S2. a) Ramp-up and ramp-down flow curves fitted to the Herschel-Bulkley model, from which a yield stress $\sigma_y \approx 0.5$ Pa is determined at rest. b) Melting and cooling curves of single and double gels at volume fraction $\phi = 0.05$. c) Strain sweeps of single and double gels at representative volume fractions. Solid lines: storage moduli G', dotted lines: loss moduli G'', arrows illustrate 'overshoots' during yielding of gels. c) critical strain γ_c and d) critical stress σ_c of bigels (green) and monogels (black: silica, red: tripalmitin) at low volume fractions $\phi \lesssim 0.1$. Dashed lines are power-law visual guides.

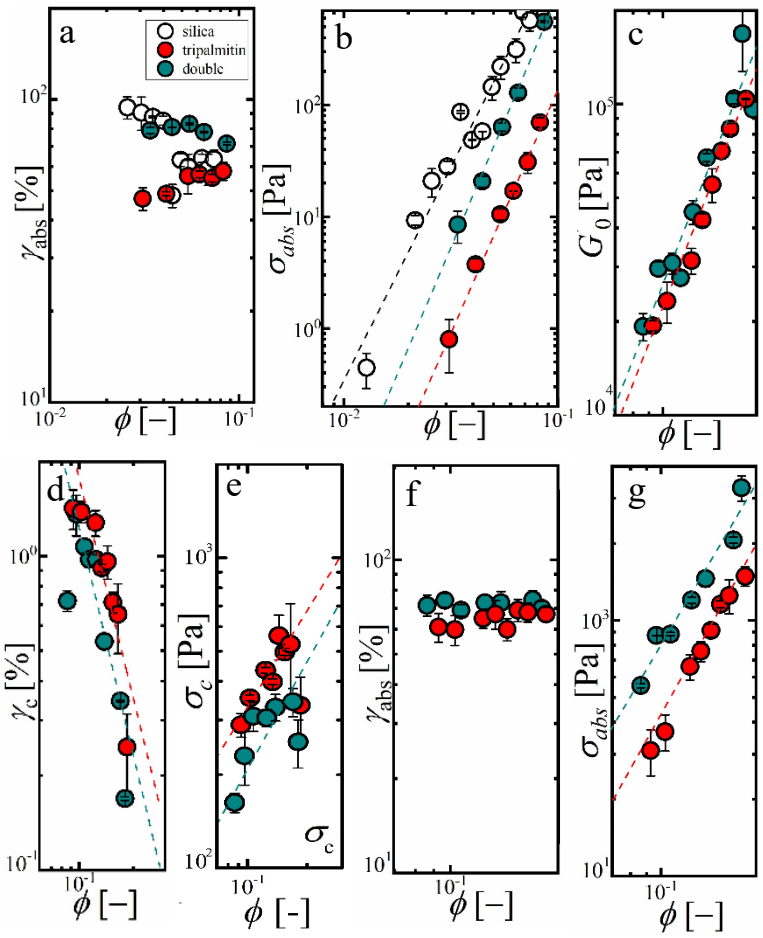

Figure S3. a) absolute strain γ_{abs} and b) absolute stress σ_{abs} at the crossover point $G' = G''$ of gels in the dilute regime $\phi \lesssim 0.1$, c) plateau modulus G_0, d) critical strain γ_c and e) critical stress σ_c at the onset of yielding, f) absolute strain γ_{abs} and g) absolute stress σ_{abs} at the crossover point $G' = G''$, in the concentrated regime $\phi \gtrsim 0.1$. Dashed lines are power-law fittings.

.

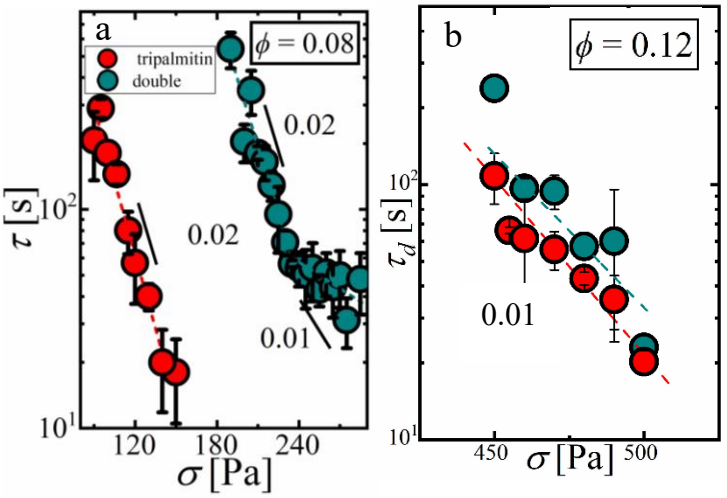

Fig. S4. Delay time τ_d between the application of the shear stress and at the moment of yield for a) dilute gels an b) concentrated gels. Lines are experimental fits to Eq. 6, and slops indicate the scaling of τ_d. Data points with error bars represent averaged quantities with their corresponding standard deviations.

Table S1. Structural parameters for various gel systems obtained from delayed yielding experiments and Eq(4); strand coarseness (n), bond "compliance" and quiescent bond dissociation and association rates . The σ_c is the critical stress separating the stress regimes

	ϕ	n [-]	C	k_D	k_A	σ_c
Silica single	0.01	1	0.70	0.23	-	-
Tripalmitin single	0.05	1	0.094	0.21	-	-
Tripalmitin single	0.08	1	0.02		-	-
Tripalmitin single	0.10	1	0.01	0.24	-	-
Tripalmitin single	0.12	1	0.009	0.16	-	-
Double gel	0.05	5.8	0.018	0.13	0.37	56.3
Double gel	0.08	5.1	0.004	0.15	0.37	221.2
Double gel	0.10	1	0.009	0.19	-	-
Double gel	0.12	1	0.012	0.13	-	-

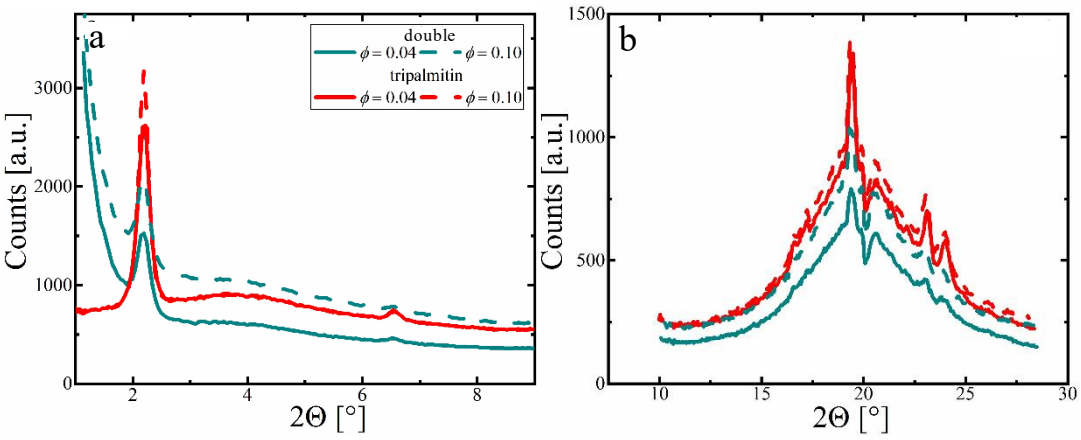

Figure S5. Representative SAXD (a) and WAXD (b) spectra of single lipid and double silica-lipid gels. and starch-lipid suspensions.

From the SAXD patterns, the chain length packing of tripalmitin or crystal thickness (τ) were estimated from the first small angle reflection corresponding to the (001) plane using the Scherrer equation:

$$\tau = \frac{K\lambda}{\beta \cos(\theta)}$$

where K is a dimensionless shape factor (0.9 for crystallites), λ is the x-ray wavelength (0.15418 nm) θ is the Bragg angle, and β is the is the full width at half Maximum (FWHM) value (in radians) of the first small angle reflection corresponding to the (001) plane (Fig. S4a).

From the WAXD patterns, peaks associated with the interchain packing or subcell structure (S) were identified. Strong lattice spacings at 4.6 Å and several other strong peaks at 3.7 Å and 3.9 Å were identified, associated with a triclinic chain packing were found.

Results are summarized in the following table:

Table S2. Crystalline thickness and subcell structure of representative lipid single monogels and double gels.

Sample	τ	S
$\phi_{\text{tripalmitin}} = 0.05, 0.10$	$38.5 \pm 0.8, 40.8 \pm 2.5$	β, β
$\phi_{\text{double}} = 0.05, 0.10$	$40.5 \pm 0.7, 42.8 \pm 4.1$	β, β

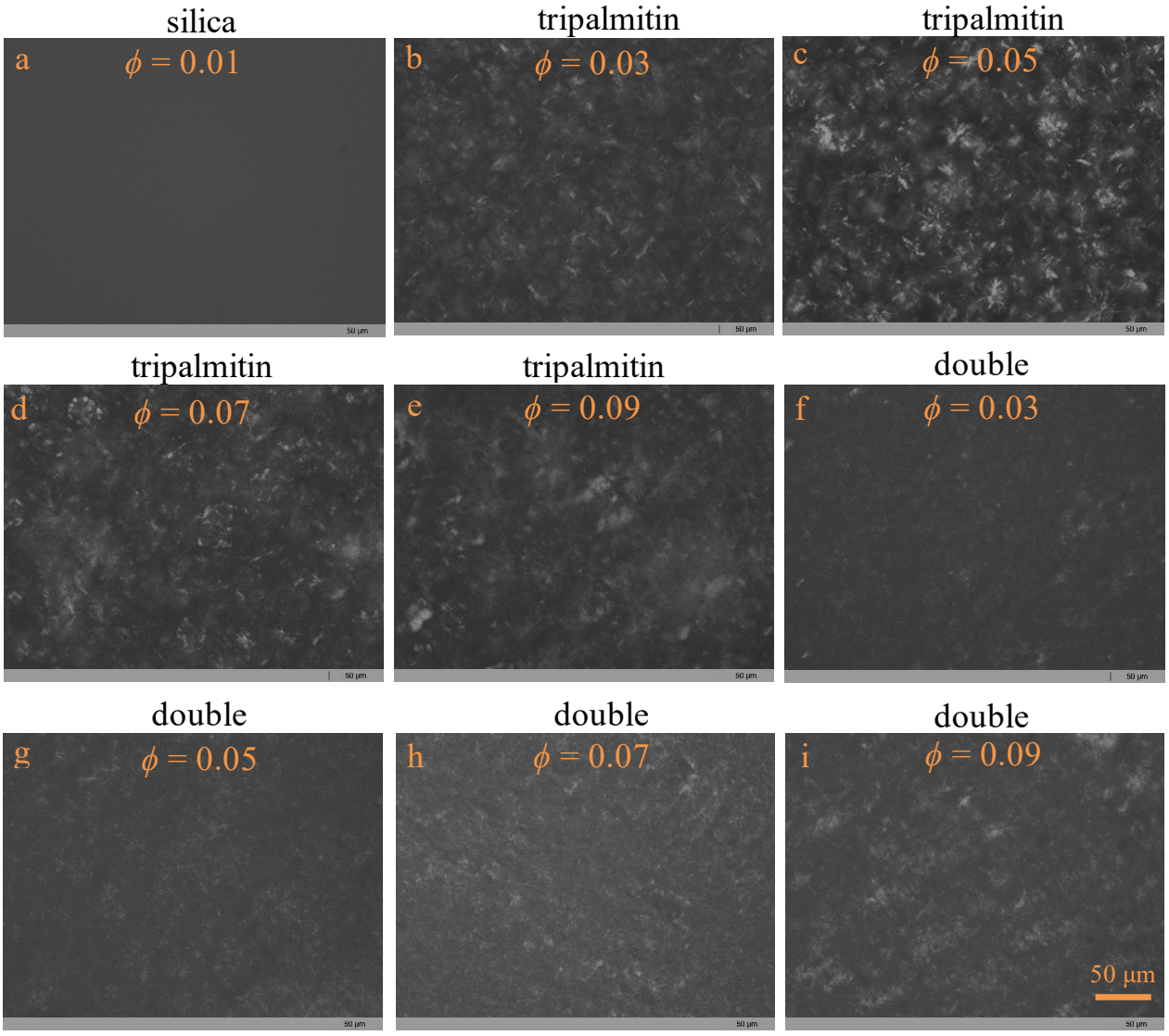

Figure S6. Polarized microscopy images of single (a-e) and double (f-i) at increasing volume fraction in the dilute regime (ϕ = 0.03-0.09). Silica and liquid oil appear black since they are amorphous. All images share the same scale bar.

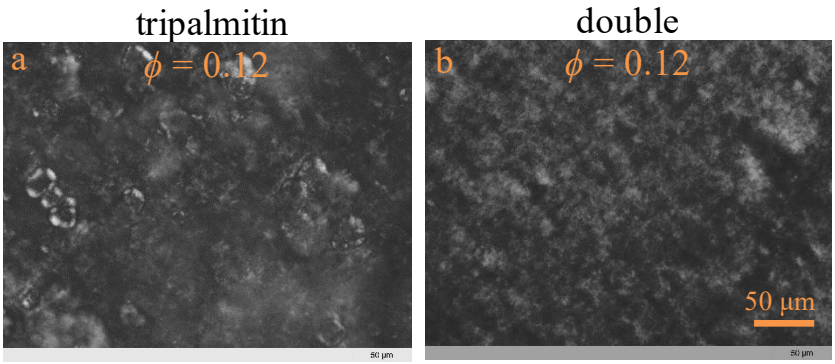

Figure S7. Polarized microscopy images of single (a) and double (b) gels in the concentrated regime (ϕ = 0.12). Silica and liquid oil appear black since they are amorphous. All images share the same scale bar.

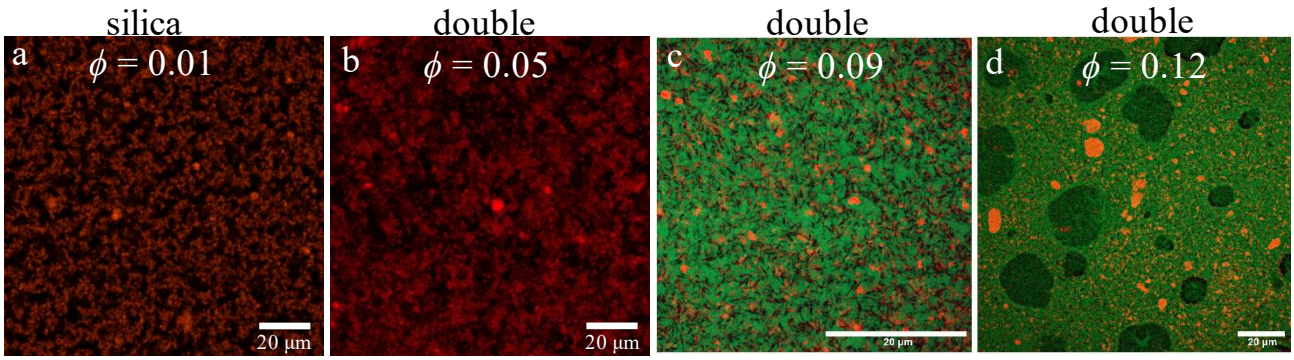

Figure S8. CLSM images of single and double gels at a) ϕ = 0.01 silica, b) ϕ = 0.05 double, c) ϕ = 0.09 double, ϕ = 0.12 double. Oil-channel including the negatively stained lipid aggregates (black) have been removed in a) and b) for better visualization of the silica gel network.